Multi-Antenna Techniques for NLoS and Spoofing Detection using Vehicular Real Signal Captures in Urban and Road Environments

E. Domínguez, J. M. López-Almansa, *GMV, Spain*;
G. Seco-Granados, J. Salcedo, D. Egea, *UAB, Spain*;
E. Aguado, D. Lowe, *NSL, United Kingdom*;
D. Naberezhnykh, *TRL, United Kingdom*;
F. Dovis, *Politecnico di Torino, Italy*;
J.P. Boyero, *European Commission, Belgium*

BIOGRAPHY

Enrique Domínguez received a M.Sc. degree in Telecommunications Engineering in 2000 and a Master in Space Technologies in 2009, both from the Polytechnic University of Madrid. He joined GMV in 2000 working first in the development of EGNOS and Galileo and since 2009 in GNSS software receivers, multi-sensor fusion algorithms and integrity algorithms.

Jose María López-Almansa holds a M.Sc. degree in Telecommunications Engineering from the Polytechnic University of Madrid. He started on GNSS as a research trainee for two years at ESA/ESTEC and joined GMV at the end of 1999, where his activities include GNSS signal processing, simulation tools and navigation and integrity algorithms.

Gonzalo Seco-Granados holds a PhD degree from Univ. Politecnica de Catalunya (UPC) and an MBA from IESE, Universidad de Navarra. Since 2006, he is associate prof. at the Dept of Telecom. Eng. of UAB and head of the SPCOMNAV group.

José A. López-Salcedo received the M.Sc. and Ph.D. degrees in Telecommunication Engineering in 2001 and 2007 from UPC. He joined UAB and the SPCOMNAV group as an assistant prof. in 2006, and since 2013 he is an associate prof.

Daniel Egea received the M.Sc. in Electrical Engineering in 2012 and the M.Sc. degree in Micro and Nano Electronics Engineering in 2013, both from Universitat Autònoma de Barcelona (UAB). Currently, he is a Ph.D. student at the SPCOMNAV group, of UAB and his research is focused on signal-level GNSS integrity.

L. Enrique Aguado is a Principal Project Manager at NSL. He received a Ph.D. in Electrical Engineering from the University of Manchester, UK. He has been involved in Galileo-related R&D since 2002 with his current work focussed on robust positioning technologies.

David Lowe is a Principal Navigation Engineer at NSL. He received a PhD in Engineering Surveying and Space Geodesy from the Univ. of Nottingham, UK. He has been involved in GNSS navigation technologies, researching GNSS for aircraft precision approach and landing, deformation monitoring, sea-level determination and land navigation with emphasis on the rail domain.

Denis Naberezhnykh received the BSc. degree in Physics from the Royal Holloway, University of London and is the Head of Low Carbon Vehicle and ITS technology at TRL. He has worked on numerous tests for the evaluation of GNSS-based vehicle OBUs.

Fabio Dovis received a Master degree in Electronics Engineering in 1996 and a PhD in Electronics and Communications Engineering in February 2000, at Politecnico di Torino. He is currently assistant professor at the Department of Electronics and Telecommunications of Politecnico di Torino. He strongly contributed to the creation of the NavSAS group. His research focuses on the design of algorithms and architectures for satellite navigation receivers.

Juan Pablo Boyero is since 2012 working at the EC in the definition of the evolution of the Galileo and EGNOS missions. Before he worked within the Galileo System Performance area and acting both as System Prime as well as Technical Support to System Prime. He holds a M.Sc. by the Escuela Técnica Superior de Ingenieros de Telecomunicación of the Universidad Politécnica de Madrid. He also passed the course on Safety Critical Systems by the University of Oxford, UK.

ABSTRACT

The use of GNSS has expanded to mass market users and most of them are located in populated areas and roads where local environmental characteristics, which include buildings, trees, moving objects, etc., increase the

multipath and the Non-Line-of-Sight (NLoS) effects, thus dominating the GNSS measurement errors. Also threats like radio frequency (RF) interference and spoofing can affect the positioning service. These local characteristics, which cannot be corrected by the ground or satellite segments, degrade the signals leading to potentially high positioning errors and therefore may also hinder the provision of a full integrity positioning service.

The purpose of the current study is to assess the possibilities that a mass-market level multi-antenna device could offer in order to improve integrity by identifying faulty measurements (i.e. high error measurements).

Using the real data collected with a GPS&GLONASS single-frequency three-antenna array in urban and road environments, the paper presents the results obtained applying several multi-antenna techniques at PVT level aimed to cope with local effects by identifying high error measurements to improve the navigation solution (meas. errors were obtained using a high quality truth reference platform and dedicated post-processing software). Thus, different multi-antenna indicators are analyzed assessing their capability of detecting high error measurements and then several combinations of indicators are used as a Fault Detection and Exclusion (FDE) and tested with a navigation algorithm in order to assess their impact on the position errors.

One of the main objectives of the study is to assess the possibility of exploiting the multi-antenna FE phase measurements to identify NLoS measurements in urban environments; this is because antenna phase differences contain information related to the direction of arrival (DoA) of the received signals, also known as angle of arrival (AoA). NLoS measurements do not usually arrive from the expected DoA, which for direct signals can be obtained from user attitude and satellite Line-of-Sight (LoS), so this turns phase differences into a potential indicator that can be used to detect NLoS.

Besides, the paper demonstrates how, only using the antenna phase differences, the presence of a spoofer can be detected when the spoofing signals arrive from the same direction. This can be done without any external info, even without calibrating the difference between the antenna HW biases.

INTRODUCTION

The paper presents the research on multi-antenna techniques at PVT level and the results obtained using the real data gathered in urban and road environments. These results have been obtained within the frame of the Integrity GNSS Receiver (IGNSSRX) project which was a European Commission funded project, developed between 2012 and 2015 by a consortium including GMV, NSL, TRL and UAB. The project had three main objectives:

a) The development of two platforms to capture and store GNSS radio frequency signal samples and a reference trajectory from representative low-, medium- and high-end sensors in terrestrial applications.
b) An extensive data collection campaign aiming to characterize error sources, magnitudes and probabilities for two important GNSS terrestrial application areas: automotive and pedestrian users.
c) The research and development of techniques and algorithms to mitigate the integrity threats in the two terrestrial environments studied using the collected data, thus allowing reliable terrestrial applications within these domains.

While the first two objectives were already presented in detail in [1], this paper is focused on the work developed on multi-antenna techniques (part of the third objective).

The multi-antenna RF samples were obtained using a three-antenna Front-End (FE) system (SRX-TRITON [2]), working in the GPS L1 and Galileo E1 band and in the GLONASS L1 band, and fed by a common oscillator. The RF samples collected by the three-antenna FE during the road and urban collection campaigns were processed with the SRX ([3]) software receiver providing pseudorange, Doppler and carrier phase measurements for each antenna. The difference between the measurements received at different antennas may contain information about the quality of the measurements, which turns them into potential indicators for detecting high error measurements. In the particular case of the carrier phase differences, they are affected by the DoA of the received signal so they can also be used as a valid indicator of NLoS measurements (when the attitude is known and the expected DoA can be computed). The use of a reference trajectory and attitude platform allowed the evaluation of the measurement and position errors.

The paper starts with a brief description of the vehicular platform and the performed data collection campaign from the multi-antenna point of view. It continues with the analysis of the multi-antenna measurements and the different indicators that can be used to detect high error measurements. Then it analyzes different multi-antenna Fault Detection and Exclusion (FDE) algorithms based on combinations of the analyzed indicators and assesses their impact on the navigation solution by analyzing the improvement in the position error statistics. Finally, the paper presents the spoofing detection capability of the three-antenna FE and provides the conclusions.

DATA COLLECTION PLATFORM

The IGNSSRX Data Acquisition and Storage Unit (DASU) is completely described in [1], the results presented in this paper were obtained using some of the Vehicular DASU elements, that is, the three-antenna FE, the CSAC clock and the truth reference (see Figure 1). Hence, only these elements will be briefly described here.

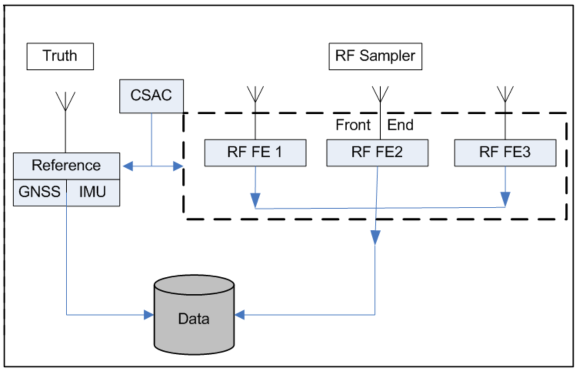

Figure 1- Overview of the Vehicular DASU elements used in the current study

The SRX-TRITON [2] is the three-antenna Front-End (FE) used in the vehicular DASU to record the multi-antenna RF samples during the collection campaign. It was configured to work in the GPS L1 / Galileo E1 and the GLONASS L1 bands with the platform CSAC clock providing the 10 MHz oscillator input common to all the FEs (Symmetricom SA.45s CSAC). The SRX-TRITON used three patch antennas (Tallysman TW2400) mounted on a frame on top of the vehicle roof. Figure 3 shows the SRX-TRITON architecture and Table 1 provides the configuration parameters used to record RF samples.

Figure 2- SRX-TRITON Three-Antenna Front End

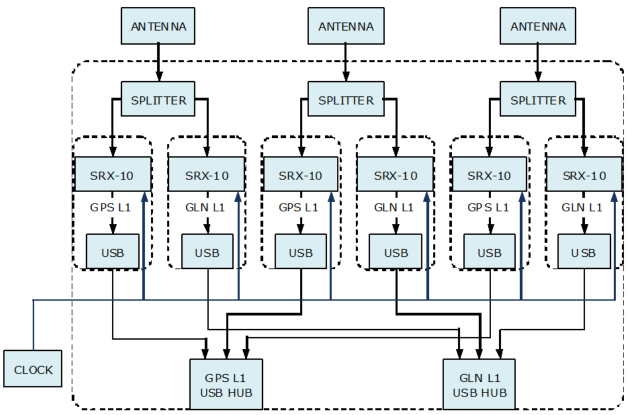

Figure 3- Vehicular DASU RF Front-Ends Architecture

SRX-TRITON Configuration for Vehicular DASU	
SRX-10 Three-antenna RFFE (DoA studies)	GPS L1 chains • IF bandwidth: 4.2 MHz • ADC quantization: 1 bit • ADC sampling rate: [10] Ms/s I • Data throughput: 3.75 MB/s GLONASS L1 chains • IF bandwidth: 9.6 MHz • ADC quantization: 1 bit • ADC sampling rate: [20] Ms/s I • Data throughput: 7.5 MB/s

Table 1- SRX-TRITON RF Front-Ends Configuration

The truth reference trajectory system in the vehicular DASU provides the reference position and attitude which allows computing the measurement and positioning errors. This truth reference system also uses the CSAC clock as input and is provided by a NOVATEL GPS&GLONASS L1/L2 with SPAN-CPT and wheel sensor:

- Novatel Micropod OEMV-3+MPPC / CPT-IMU / GPS-702-GG antenna
- Corrsys-Datron WPT1000 Incremental Wheel Pulse Transducer (DMI) for test car

DATA COLLECTION CAMPAIGN

A detailed description of the IGNSSRX data collection campaigns can be found in [1]. The results presented in this paper are based on the vehicular data collection campaign which consisted on repeating two different routes, road/motorway and urban:

- *Road/Motorway*: the route starts from TRL's office and goes along M4 as shown in Figure 4, is 92km in length and takes 64 minutes in free flow traffic.
- Urban: consists on a city drive in London from Hammersmith towards Tower Bridge and returning back to Hammersmith, as shown in Figure 5, with urban canyons and a 300 meter tunnel. It is 24km in length (59 minute drive in free flow conditions; 2 hours 30 minutes due to start-stop traffic).

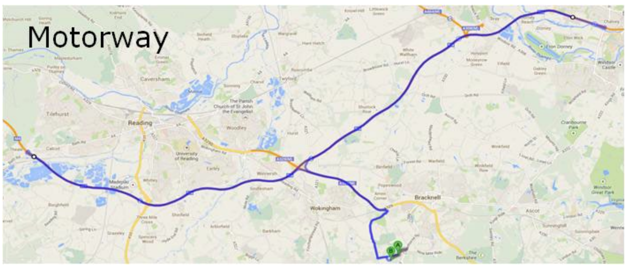

Figure 4- Vehicle Data Collection: London Motorway route

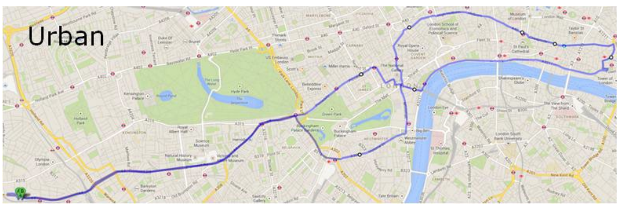

Figure 5- Vehicle Data Collection: London Urban route

The three antenna array is formed by the MASTER (M), SLAVE1 (S1) and SLAVE2 (S2) SRX-TRITON antennas, thus, providing three different baselines (being the third one redundant) and forming the first two baselines a right angle (see Figure 6):

- Baseline1: SLAVE1 – MASTER
- Baseline2: SLAVE2 – MASTER
- Baseline3: SLAVE2 – SLAVE1

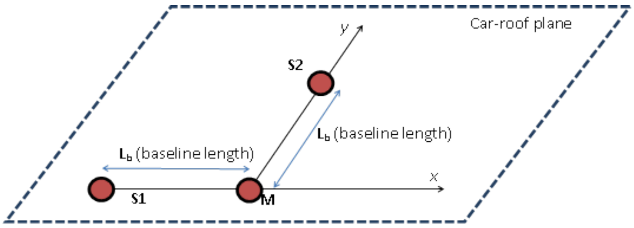

Figure 6- Three antennas disposition on top of the car roof

Three subsets of data were collected from the distance between antennas point of view, one with an antenna separation of λ/2, other at λ and a third one at 2λ (GPS L1 λ). From the angle estimation point of view, as the distance between the antennas increases, the number of ambiguities in the estimated angles also increases and the angle estimation error is reduced. On the other hand, the noise and the characteristics of the collected carrier phase measurements are the same independently on the separation of the antennas, so the current analysis is based on data recorded with a distance of λ/2 (GPS L1 λ) between the antennas of the first two baselines.

A spoofing scenario was also tested at the EC Joint Research Centre (JRC) in Ispra (Italy) with the three-antenna FE and the same antenna configuration to provide data to test the spoofing detection algorithm based on the direction of arrival of the spoofing signals, which would all come from the same direction. Thus, in order to simulate spoofing at the JRC EMSL anechoic chamber, the GNSS signals received by an antenna placed on the roof were re-broadcast inside the anechoic chamber using a single transmitter. The GNSS signals were sampled using the SRX-TRITON Three-Antenna FE ([2]) placed within the anechoic chamber and configured with an antenna separation of λ/2. Coming from the same source within the anechoic chamber, all the re-broadcast signals arrive to the FE antennas from the same direction.

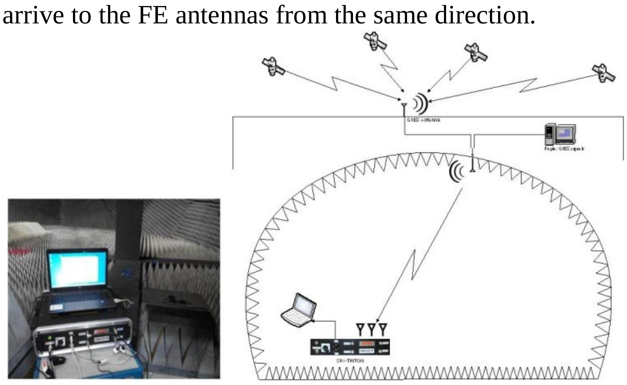
Figure 7- Spoofing test set-up

MULTI-ANTENNA MEASUREMENTS

The three-antenna FE [2] with a common clock used in the vehicular DASU and the SRX [3] receiver provide measurements from three different antennas placed on top of the car with a fixed and known separation between them. These extra measurements (compared with a single antenna receiver) could be used for different purposes. As the IGNSSRX project is focused on integrity, the first objective is to analyze the information provided by these extra measurements and their relation with measurement errors in order to assess the possibility of using them to detect the faulty measurements so they could be ignored (FDE) or down-weighted in the navigation process, thus, reducing the errors and improving the availability and the integrity performances.

In an ideal configuration and in a clean environment the measurements received at each antenna should be the same except for the effect caused by the separation between the antennas. Hence, the analysis performed will be based on the differences between the measurements received at each antenna. The following measurement differences between antennas will be analyzed:

- Carrier-Phase Differences
- Pseudorange Differences
- Doppler Differences

CARRIER PHASE DIFFERENCES

Generation of Carrier Phase Measurements

The generation of Carrier-Phase measurements is a process weaker than the pseudorange generation. Especially in urban environment and car applications, the PLL usually works under severe stress, being quite sensitive to low-power signals, transient conditions, etc. SRX ([3]) allows the user to select between two different implementations of PLL discriminators for carrier-phase tracking loop:

- **Costas-Loop ATAN PLL** ("stand-alone"):
  - Advantage: it allows carrier-phase tracking on bit-modulated signals with no assumption of the specific value (1/-1) or the bit.
  - Drawback: it produces carrier phases with half-wavelength ambiguities (~8.5cm), whose resolution requires synchronization with the GPS preamble (transmitted every 6 seconds). Half-cycle ambiguity appears at initialization and when the CP tracking is lost and recovered (quite frequent in car applications and in urban).

- **ATAN2 PLL**: In case that the signal does not include bit modulation (pilot) or if the bits can be wiped-off (see section 5.3.1 of [4]), the PLL can use an ATAN2 discriminator, which does not suffer from half-cycle ambiguity. ATAN2 PLL implies an improvement of

6 dB with respect to ATAN PLL (see last paragraph in "Phase Lock Loops" section 5.3.1 of [4], page 166).

- SRX allows two "wiping-off" mechanisms:
  - Stand-alone: initially, Costas ATAN PLL is used in order to decode a full superframe (750 s), which will be used with the ATAN2 PLL during its validity period.
  - Bit-true assistance: the bit sequence is provided externally.
- Knowing the bit sequence, the SRX wipes off 92% of the bits (due to reserved bits). When the bits are not wiped-off ATAN PLL is used, so half-cycle ambiguities could still appear.

In order to avoid the half-wavelength ambiguities, the phase results presented in this paper have been obtained using the wiping-off capability of the SRX (to avoid half-wavelength jumps in phase differences the important thing is to use/decode the same bits in the different PLLs).

The SRX generates a valid carrier phase measurement when the phase lock indicator, internally computed in the tracking process, is above a certain threshold. SRX employs the $c2\phi_k$ described in chapter 8.IV.G.3 of [5]:

$$c2\phi_k = \frac{NBD_k}{NBP_k} \quad ;$$

$$NBD_k = \left(\sum_{i=1}^{M} I_i\right)_k^2 - \left(\sum_{i=1}^{M} Q_i\right)_k^2 \quad ;$$

$$NBP_k = \left(\sum_{i=1}^{M} I_i\right)_k^2 + \left(\sum_{i=1}^{M} Q_i\right)_k^2$$

A typical threshold of 0.8 has been used in the analysis of double difference carrier phase residuals. As expected, the availability of carrier phase measurements is reduced in urban environment, so a permissive threshold of 0.4 has been used to perform the single difference carrier phase analysis, thus increasing the phase noise but allowing a better characterization and study of what can be achieved.

Carrier Phase Differences

This section explains how to use the carrier phase (CP) differences to provide useful information for measurement error detection. The CP differences between antennas can be potentially exploited for fault detection purposes regarding, at least, against to two main threats:

- NLoS
- Spoofing

The underlying concept is based on using the CP differences to compare the direction of the received signal with the expected directions, obtained from the user attitude and satellite Line of Sights (LoS).

Figure 8 presents a configuration with two antennas (1 and 2) forming a baseline vector $\overline{b}_{1,2}$. Then, the angle α between both can be defined in terms of the scalar product, as the projection of the baseline on the LoS:

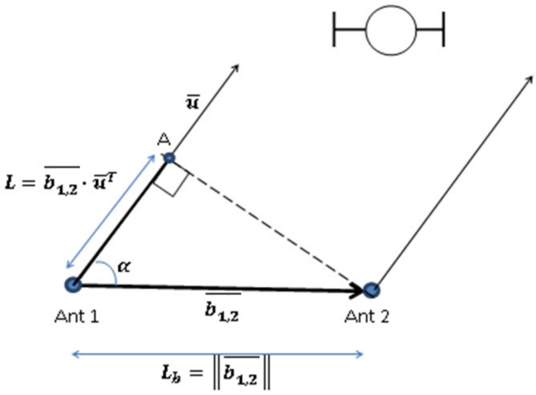

Figure 8- DoA estimation with two-antennas

$$\alpha = \mathrm{acos}\left(\frac{L}{L_b}\right) = \mathrm{acos}\left(\frac{\overline{b_{1,2}} \cdot \overline{u}^T}{\left\|\overline{b_{1,2}}\right\|}\right)$$

L can be expressed as the difference between the GNSS true ranges of both antennas (R_1 & R_2) since Antenna 2 and point A (on the Antenna-1 LoS) are at the same wavefront:

$$L \equiv \Delta R_{1,2} = R_1 - R_2 = \left\|\overline{b_{1,2}}\right\| \cdot \cos(\alpha)$$

In order to estimate angle α based on GNSS technology, the measurements (observables that estimate the values R_1 & R_2) should provide an accuracy much better than the characteristic lengths involved (related to the baseline distance). For this purpose, pseudoranges would be useless, since they are too noisy compared with the baseline lengths used in the vehicle campaign ($\lambda/2$, λ and 2λ). Angular estimation with GNSS is generally achieved based on carrier phase observables, which are much more accurate (cm level). Also, this angular estimation is usually performed by estimating the phase integer ambiguities, but in the current context the resolution or estimation of the ambiguities would be very difficult because the FE is single frequency (the platform wants to be representative of current mass market receivers), because of the short antenna baselines that can be employed on top of a car and due to the high noise level and frequent cycle slips present in urban environment. Besides, the algorithm should be standalone so no reference station can be used. Hence, the angular estimation will be based on the fractional part (λ-module) of the carrier phase differences to get rid of the integer ambiguities.

By performing the CP single differences between two antennas ($\Delta\varphi_{1,2}^j = \varphi_1^j - \varphi_2^j$) the common errors (tropo, iono, satellite orbit and clock) cancel out and the following measurement model can be defined for satellite *j*:

$$\Delta\varphi_{1,2}^j = \Delta R_{1,2}^j + \Delta\tau_{1,2} + \lambda \cdot \Delta N_{1,2}^j + SyncrhoErr_{1,2}^j + noise_{1,2}^j$$

where:

- $\Delta R^j_{1,2}$ is the difference between the true ranges and it is related to the angle α (see Figure 8):
- $\Delta\tau_{1,2}$ is the difference between receiver clocks. As the FEs use the same clock oscillator, this term would only be affected by differences in the clock realization at each FE ($\Delta clk_{1,2}$) and by differences between the HW bias at each antenna&FE chain ($\Delta HW_{1,2}$):

$$\Delta\tau_{1,2} = \tau_1 - \tau_2 = \Delta clk_{1,2} + \Delta HW_{1,2}$$

- $\lambda \cdot \Delta N^j_{1,2}$ is the differential integer ambiguity.
- $SyncrhoErr^j_{1,2}$: if phase measurements had been taken at different moments this affects phase differences and the impact would be different for each satellite *j*:

$$SyncrhoErr^j_{1,2} = \Delta t_{sync_{1,2}} \cdot (\vec{v}^j_1 + clkDrift) = \Delta t_{sync_{1,2}} \cdot Dopp^j$$

- $noise^j_{1,2}$: noise difference between antennas 1 and 2 (it includes multipath).

Therefore, the impact of some of the terms modelling $\Delta\varphi^j_{1,2}$ will depend on the FE (SRX-TRITON [2]) and on the receiver used to generate the measurements (SRX [3]). Hence the following platform aspects should be taken into account:

- The clock used by the FEs is a very stable clock (CSAC) with a very low clock drift.
- The SRX synchronizes the generation of the measurements down to tens of nanoseconds at the beginning of the processing (during 10 ns a satellite can move up to around 40 µm) and leaves this synchronization constant during the whole execution.
- Each antenna RF chain is equal to the other (same components and same cable lengths) but manufacture differences or temperature differences could lead to non-zero HW bias differences. Nevertheless, the difference of HW bias should be stable enough
- The same FE chips are used with a common input clock oscillator, but they use an independent up-conversion of the local clock to L1, as a result, although the clock is common, the local carrier is generated at each FE with a random initial phase offset. One may think that these differences should be constant, but they could potentially slowly rotate due to thermal noise in the synthesizer PLL (wander). Moreover, due to manufacturing differences and/or temperature variations, the intensity of this phase wander process may vary between FEs.

The first two points ensure that the synchronization error will have a negligible effect and the last three that the difference between the receiver clocks ($\Delta\tau_{1,2}$) is a term common to all the satellites using the same λ that can be modelled as an initial bias different from zero that slowly varies with temperature and time. Hence, taking this into account, the fractional part (λ-module) of $\Delta\varphi^j_{1,2}$ can be represented as:

$$mod_\lambda\left(\Delta\varphi^j_{1,2}\right) = mod_\lambda\left(\left\|\overline{b_{1,2}}\right\| \cdot \cos(\alpha^j) + \Delta\tau_{1,2} + noise^j_{1,2}\right)$$

At this point there are two ways to cope with this bias term ($\Delta\tau_{1,2}$):

a) Perform double differences (DD) using a pivot satellite (with the same λ):

$$\nabla\Delta\varphi^{i,j}_{1,2} = \Delta\varphi^i_{1,2} - \Delta\varphi^j_{1,2}$$

$$mod_\lambda(\nabla\Delta\varphi^j_{1,2}) = mod_\lambda\left(\left\|\overline{b_{1,2}}\right\| \cdot \left(cos(\alpha^i) - cos(\alpha^j)\right) + noise^{i,j}_{1,2}\right)$$

the drawback is that each "differencing" level increases the uncorrelated noise (by a factor of√2 if noise is Gaussian). This fact becomes important in urban where noise increases due to local effects.

b) Use the single differences (SD) after calibrating the bias term taking into account that it is common to all satellites and that it varies very slowly with time.

$$Calibrated\{mod_\lambda(\Delta\varphi^j_{1,2})\} =$$

$$= mod_\lambda\left(\left\|\overline{b_{1,2}}\right\| \cdot cos(\alpha^j) + (\Delta\tau_{1,2} - \widehat{\Delta\tau_{1,2}}) + noise^j_{1,2}\right)$$

the bias term can be calibrated using the expected satellite LoS and the user attitude, for example provided by the navigation algorithm (by averaging measurements of different satellites and through different epochs).

Hereafter, the results obtained in real road and urban environments with carrier phase double differences (DD) and single differences (SD) will be presented. As the measurements used for the pivot satellite in DD and for calibrating the bias in SD require to have the same λ, then only GPS measurements will be taken into account. GLONASS satellites are transmitted at different frequencies so each one may have a different initial CP SD bias (evolution should be common to all sats).

CP Double Differences (DD)

With the DD the bias term is removed and the resulting $\nabla\Delta\varphi^{i,j}_{1,2}$ will only depend on the DoA of the two satellites used in the DD. Also the noise is increased with the DD, the noise of the pivot satellite will be added to all DD measurements. Hence, the satellite with higher elevation or higher C/N0 is usually selected as pivot satellite for performing the DD.

The actual DoA of the satellites can be computed using the truth reference data provided by the platform (user position and attitude), so the effect of the satellite DoA can be removed from the CP DD obtained with real data, thus obtaining the CP DD residuals, which are representative of the CP DD measurement errors.

Figure 9 and Figure 10 show the obtained CP DD residuals in road and urban environments respectively, for the two different PLLs previously described (Costas ATAN PLL and ATAN2 PLL) in order to show the improvement achieved with the bit wipe-off functionality.

Three meaningful parts can be identified in the road CP DD showed in Figure 9: static at the beginning; strong foliage, when the car starts moving it follows a road that goes through a deep-forest; and open motorway. Being static, both PLLs show similar performances, but the ATAN2 PLL is more robust and provides better availability than ATAN PLL under tree canopy attenuation and in open motorway.

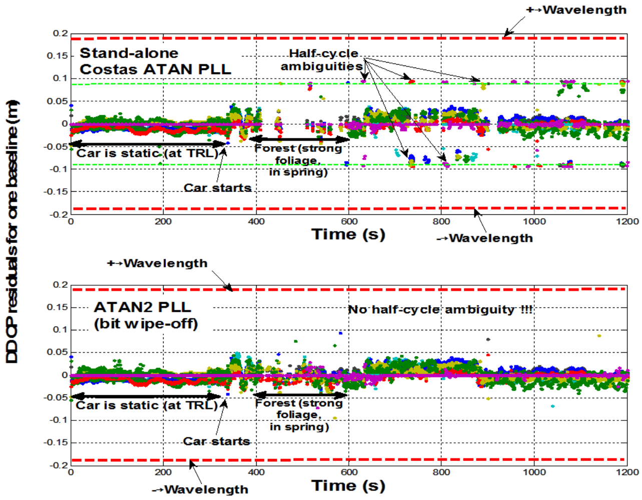

Figure 9- DD Carrier Phase Residuals - Road

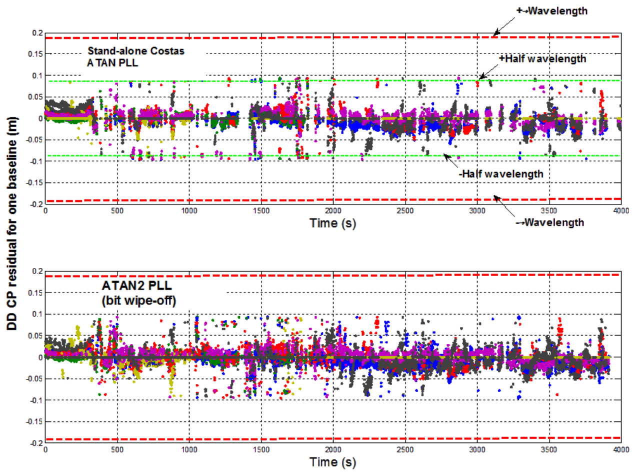

Figure 10- DD Carrier Phase Residuals - Urban

As shown in Figure 10, urban CP DD are noisier than in road environment, a cloud of significant errors appear in the order of several cm ($\pm\lambda/2$ is the working range). Also here, the wipe-off ATAN2 PLL significantly outperforms the availability of the stand-alone ATAN PLL (25-30% more measurements with ATAN2 PLL).

CP Single Differences (SD)

Calibration of CP SD

Figure 11 shows the module of the measured carrier phase single differences obtained at the laboratory in a zero-baseline configuration (the two FEs forming the baseline are fed by the same antenna) with a static antenna in an open sky environment. This zero-baseline test shows an initial bias with a very low drift (close to zero µm/s) and a slightly increasing noise along time, probably due to the rise in temperature of certain components.

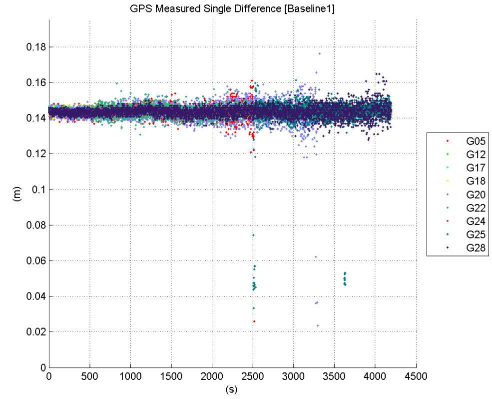

Figure 11- CP SD in zero-baseline test – Open-Sky

As stated before, in real short baseline scenarios, like the ones recorded during the collection campaign, the measured CP SD will be affected by the satellite DoA and by a bias term. Knowing the actual attitude provided by the truth reference platform, it is possible to compute the angle of arrival and thus to obtain the expected CP SD (fractional part: λ-module). Hence, the residuals can be obtained by subtracting this expected CP SD to the measured one and taking its fractional part (λ-module). These residuals are representative of the bias and CP SD measurement errors.

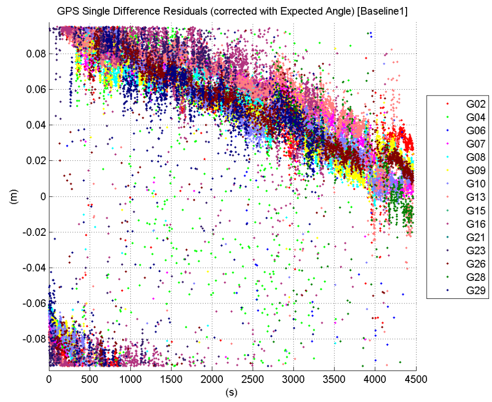

Figure 12- CP SD Residuals at Baseline1 - Road

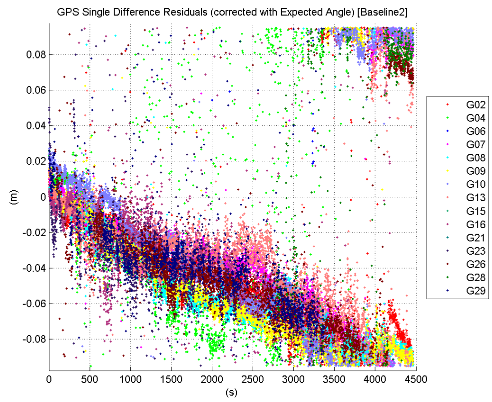

Figure 13- CP SD Residuals at Baseline2 - Road

Figure 12 and Figure 13 show the module of the residuals of the carrier phase single differences measured at each baseline obtained in a road scenario. The CP SD bias, which as expected is common to all satellites, is not zero and presents a drift (~-20 μm/s) similar in both baselines (i.e. there is a difference between the CP provided by the MASTER antenna&FE and the ones provided by the SLAVE1 and SLAVE2 antenna&FEs).

Other tests were analysed and it has been noted that, while some of them present a similar drift in baselines 1 and 2, others present a much lower drift (between -1 and +3 μm/s) similar to the one measured at the laboratory in the zero-baseline configuration. On the contrary, analyzing the third baseline in different tests, the drift is always very low (±2 μm/s) meaning that SLAVE1 and SLAVE2 differences are always very stable.

Being unlikely that differences in the HW biases could cause such almost constant drift and having checked that GLONASS CP SD residuals do not present the same drift when it appears in GPS CP SD (both share the same antennas, cables and RF splitters), then the conclusion is that the drift is caused by manufacturing differences between the MASTER FE and the SLAVEs FEs leading to a wander effect that arises due to temperature conditions that were not the same in the laboratory and in the tests where the drift was low.

Independently on the size of the bias drift, what is important is to be able to cope with the bias it in order to use the CP SD as a valid indicator. Hence, this slowly changing offset common to all satellites ($\Delta\tau_{1,2}$) needs to be removed/calibrated.

In a context where the attitude is provided by, for example, an hybrid navigator, it is feasible to obtain the carrier phase single difference residuals as in Figure 12 and Figure 13 and estimate/filter the offset over time, i.e. by taking the median of the residuals and feeding a Hatch filter to provide the offset to be removed from the residuals. Thus, this offset estimation process will be robust against faulty measurements.

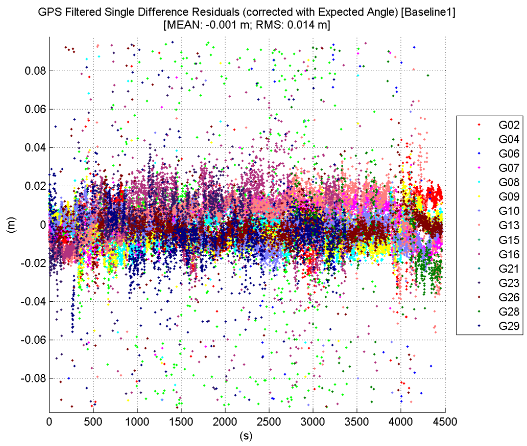

Figure 14- Filtered CP SD Residuals at Baseline1 - Road

Figure 14 shows the filtered residuals from Figure 12, it can be noted that the filtered residuals have small offsets and abrupt changes per satellite, and these small changes are correlated with changes in the attitude. Hence, these small errors are caused by errors in the baseline configuration and/or by differences in the displacement of the antenna phase centre depending on the DoA of the satellite signal. The antennas used with the TRITON FE were mass market type antennas (Tallysman TW2400 patch antennas) and their performance is not as good as the geodetic antennas in terms of centre of phase stability.

Figure 15- Patch antennas used with the TRITON FE - Tallysman TW2400

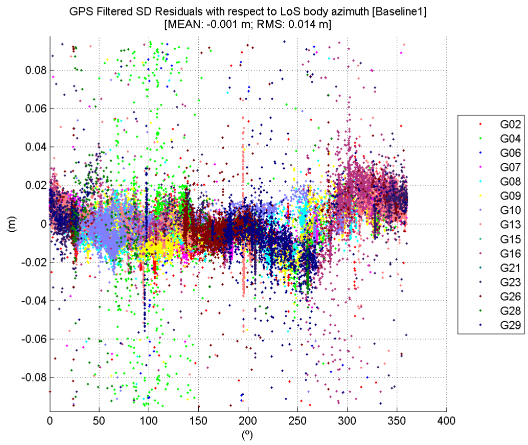

Figure 16- Filtered CP SD Residuals vs. Body Azimuth (Baseline1) - Road

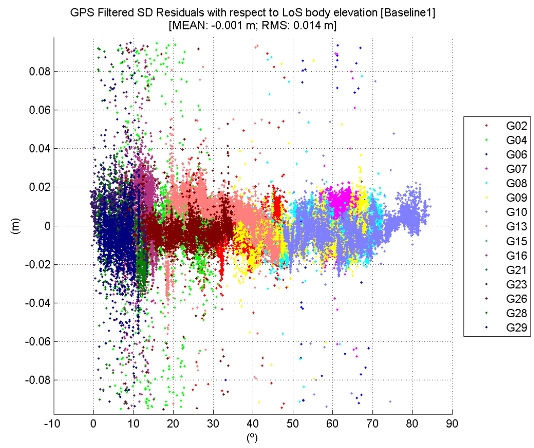

Figure 17- Filtered CP SD Residuals vs. Body Elevation (Baseline1) - Road

Figure 16 and Figure 17 show the filtered residuals against the body azimuth and the body elevation and it can be noted that the residuals depend on the DoA (azimuth and elevation in body coordinates). This dependence can be calibrated so an azimuth-elevation correction map was generated for each baseline using the residuals obtained in one road scenario (taking the mean values for each azimuth and elevation interval and interpolating them to obtain the values in intervals with low number of measurements) and used to correct the phase differences in the road and urban scenarios.

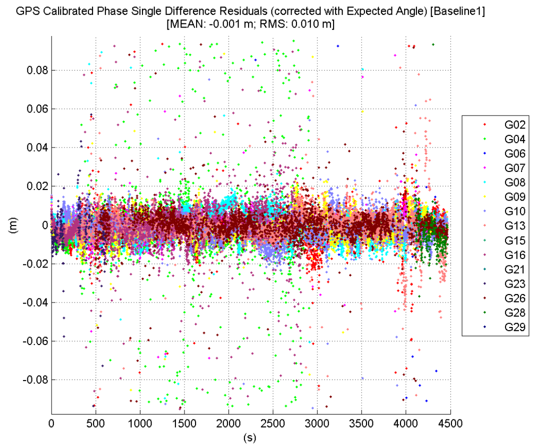

Figure 18- Corrected and Filtered CP SD Residuals at Baseline1 - Road

Figure 18 shows the filtered residuals corrected with the generated body azimuth-elevation correction map. Comparing the residuals before and after the antenna correction, the CP SD residual RMS improves from 14-15mm to 10-11mm. Reducing the RMS is very important in order to be able to set a feasible threshold in an FDE, moreover in urban where noise is higher.

This dependence adds a new term into the CP SD measurement model to cope with variations in the centre of phase between the baseline antennas depending on the DoA:

$$\mathrm{mod}_\lambda\left(\Delta\varphi_{1,2}^{j}\right) = \mathrm{mod}_\lambda\left(\left\|\overline{b_{1,2}}\right\| \cdot \cos(\alpha^j) + \Delta\tau_{1,2} + \mathrm{AntennaOffset}_{1,2}\left(\mathrm{BodyAz}^j, \mathrm{BodyEl}^j\right) + \mathrm{noise}_{1,2}^{j}\right)$$

Which assuming an ideal calibration would become:

$$\mathrm{Calibrated}\{\mathrm{mod}_\lambda(\Delta\varphi_{1,2}^{j})\} = \mathrm{mod}_\lambda\left(\left\|\overline{b_{1,2}}\right\| \cdot \cos(\alpha^j) + \mathrm{noise}_{1,2}^{j}\right)$$

Characterization of CP SD

In road environment the calibrated (i.e. corrected and filtered) CP SD residuals typically presented an RMS of around 1.1 cm and an averaged availability of 87% (100% means that for all the satellites tracked at the MASTER antenna there is an available CP SD measurement).

With respect to urban environment, the calibrated (i.e. corrected and filtered) CP SD residuals typically present an RMS of around 2.3 cm and an averaged availability of 71%. See urban CP SD residuals in Figure 19 (the gap is caused by the tunnel in the urban route),

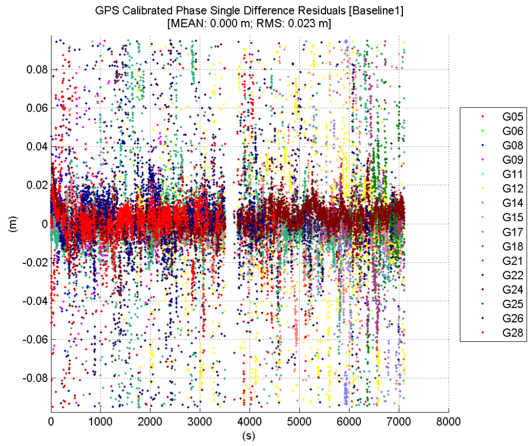

Figure 19- Corrected and Filtered CP SD Residuals at Baseline1 - Urban

Therefore, two indicators have been identified in the phase analysis:

- The availability of CP SD
- The CP SD residual obtained using attitude information

Between the CP SD and the CP DD, it has been decided to use the SD as they have lower noise than the DD and it has been demonstrated that they can be calibrated (assuming the attitude is provided or estimated).

DoA Analysis with CP SD

It is feasible to estimate the angle of arrival at each baseline using the calibrated carrier phase single differences:

$$\hat{\alpha}^j = \mathrm{acos}\left(\frac{\mathrm{Calibrated}\{\mathrm{mod}_\lambda(\Delta\varphi_{1,2}^{j})\} + \mathrm{n}\lambda}{\left\|\overline{b_{1,2}}\right\|}\right)$$

where the parameter *n* can take any integer value as long as the acos function can be computed (argument between -1 and 1).

For baselines equal or less than λ/2 there will be only one solution $\hat{\alpha}^j$, while for longer baselines the number of solutions will increase (there will be ambiguities in the angle estimation). Also note that the $n\lambda$ term and the acos argument range (between -1 and 1) can lead to "jumps" in the estimated angle due to noise. Thus, with a separation of λ/2 when the real angle is close to 0º or 180º the noise can make the estimated angle to jump between values close to 0º and 180º (estimated in the opposite direction).

The error in the estimation of the angle depends on the noise of the CP SD, on the baseline length (lower angle errors for longer baselines but in exchange of more angle ambiguities) and on the value of the angle of arrival (because the relation between the phase and the angle is not linear, it is driven by the "*acos*" function, thus, when the CP SD is close to zero for DoA around 90º the angle error will be less than for DoA close to 0º or 180º).

Therefore, in order to detect signals not coming from the right direction, it is easier to set a threshold for the phase SD measurements instead of working in the angle "domain".

The conclusion is that the three-antenna Front-End can be used to successfully estimate the DoA of the received signals using the calibrated CP SD. The performance of the AoA estimation degrades in urban as the availability of CP SD is reduced. Figure 20 provides an example of the estimated DoA.

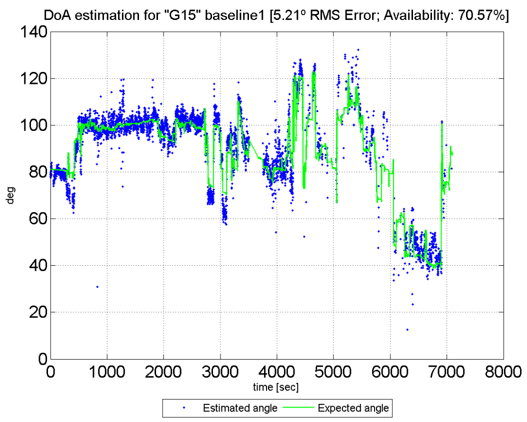

Figure 20- Example of Estimated DoA using Calibrated CP SD - Urban

The CP SD are calibrated using the attitude, this attitude information could be provided by the navigator, but due to the relation between the phase differences and the AoA there is also the possibility of computing the attitude using the CP DD measurements (for example, in epochs with enough measurements a coarse attitude can be computed using the CP DD measurements, update the slowly varying bias of the CP SD using this coarse attitude, and then use the CP SD to estimate the angles and refine the attitude).

PSEUDORANGE DIFFERENCES

This section analyzes the pseudorange (PR) differences between antennas. The measurement model for the PR SD is similar to the one described for the CP SD but without ambiguities and a higher measurement noise (includes multipath and NLoS), which means that for very short baselines, like the ones we have on top of the vehicle, the effect of the angle of arrival into the PR SD is well below the noise and will not have an appreciable impact on it. The same happens with other cm level effects like the difference between HW biases or the change of the centre of phase depending on the angle of arrival. Besides the noise, the only term that affects the PR SD measurements is the difference between the antenna clocks ($\Delta clk_{1,2}$), which can be easily estimated because the three-antenna FE uses a common oscillator so the difference can be considered constant and the SRX adjusts the difference at the beginning to be as low as possible.

$$\Delta PR^{j}_{1,2} = \Delta clk_{1,2} + PRnoise^{j}_{1,2}$$

The idea of using the PR SD as an indicator of high measurement errors consists in that if there is a great difference between the PR provided by two close antennas or if a valid PR cannot be generated at one of the antennas that would probably be indicating the presence of a strong multipath that could be introducing high errors into the navigation algorithm.

The SRX provides valid pseudorange and Doppler measurements using the same criteria for both, which is based on the measured C/N0 (valid when C/N0 is above certain configurable threshold, typically set to 20 dBHz). A PR SD is considered valid when valid PRs are provided for both baseline antennas. The PR SD measurements have a high availability (97-98%). The following figures show examples of PR SD measurements in road and urban environments:

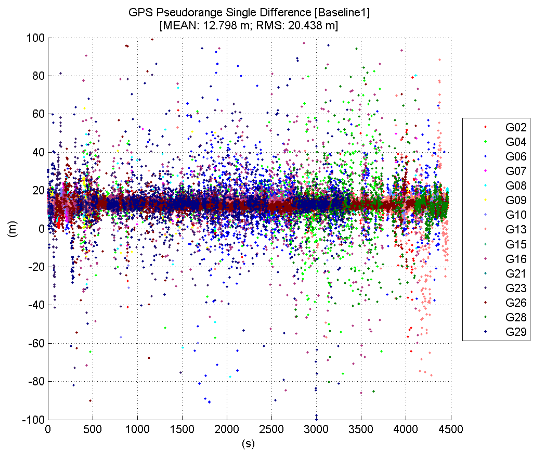

Figure 21- PR SD - Road

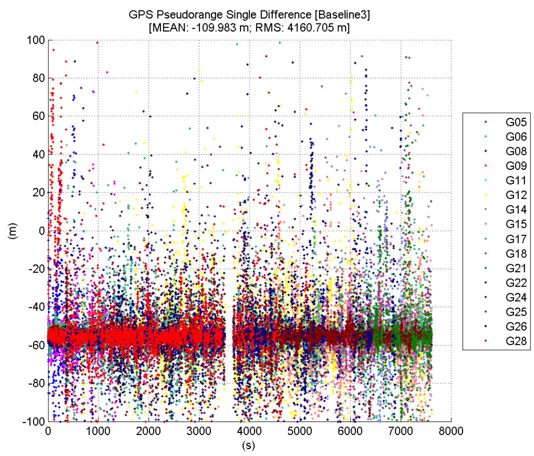

Figure 22- PR SD - Urban

DOPPLER DIFFERENCES

This section analyzes the Doppler (DP) differences between antennas. As the three-antenna FE uses a common oscillator the clock drift will be the same for the three FEs and the Doppler single differences will depend on the Doppler noise, which includes multipath, and on the velocity differences due to attitude changes but, as the distance between antennas is very short and taking into account vehicle dynamics, attitude changes will not have an appreciable impact on the Doppler differences.

$$\Delta DP_{1,2}^{j} = DPnoise_{1,2}^{j}$$

When there is a great difference between the Doppler measurements provided by two close antennas or when a valid DP measurement cannot be generated at one of the antennas that could indicate the presence of strong multipath, so DP SD and its availability can be used as indicators for detecting faulty measurements. The SRX provides valid Doppler measurements when the measured C/N0 is above certain threshold, the same criteria followed for pseudorange measurements, so they have the same availability. The following figures provide examples of DP SD measurements in road and urban environments:

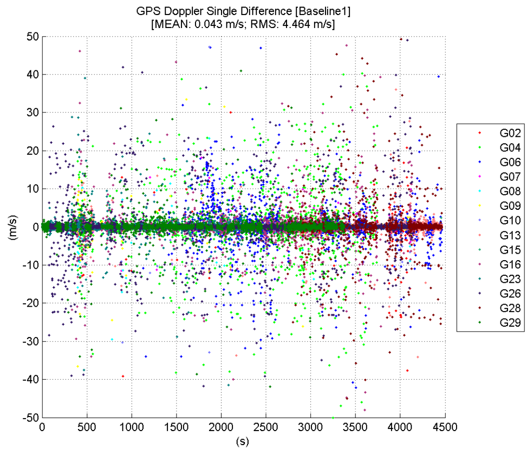

Figure 23- DP SD - Road

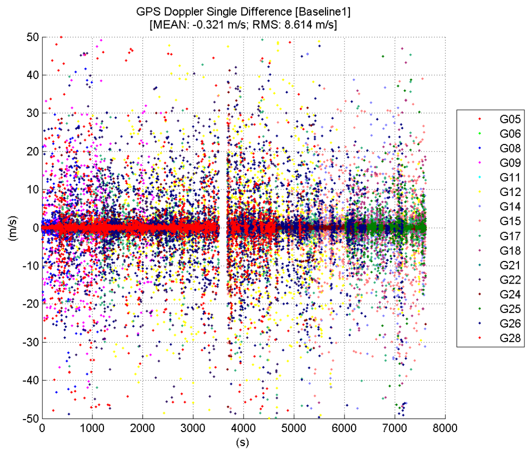

Figure 24- DP SD - Urban

MULTI-ANTENNA FDE

The purpose of this section is to analyse the possibilities offered by the multi-antenna as a Fault Detection and Exclusion (FDE) algorithm capable of detecting faulty measurements that degrade the navigation and integrity performances.

The analysis will begin assessing the Probability of False Alarm (PFA) and Probability of Missed Detection (PMD) performances of the multi-antenna indicators identified in previous sections and then different combinations of indicators will formed and tested analyzing their performances and also analyzing their impact on the Horizontal Position Error (HPE) by excluding the identified faulty measurements from the ones provided to a hybrid navigation algorithm.

It should be taken into account that the "optimal" combination of indicators for an FDE depends on the employed navigation and integrity algorithm: reducing the number of available satellites would not have the same impact on a navigation algorithm only based on GNSS measurements than on an hybrid algorithm that also uses information provided from external sensors; also, once a potential faulty measurement is identified by the FDE, for some navigation and integrity algorithms it would be better to exclude it while for others it would be better to downweight it.

Analysis of Multi-Antenna Indicators

The analysis performed in previous sections has provided the following useful indicators:

- Availability of PR&DP SD
- PR SD (after removing the clock offset)
- DP SD
- Availability of CP SD
- Calibrated CP SD residual (only GPS)

A threshold will be used over the CP SD residuals, PR SD and DP SD to decide whether the measurement should be marked as faulty (i.e. high error) or not.

The objective is to use these indicators in order to detect as much high error measurements as possible while minimizing the number of good measurements being rejected. Achieving a high availability is very important in urban scenarios as there will be streets with very few satellites in view, even when working with two constellations.

Measurement errors have been estimated using the Measurement Error Computation tool (developed within the IGNSSRX project, see [1]) which uses the position and velocity information provided by the truth platform, the IGS orbits and the IONEX ionospheric data.

In order to talk about detecting high errors, first it is needed to define which errors are considered high. For a first analysis the following arbitrary thresholds will be used to separate between good and faulty measurements to compute the PFA and PMD statistics:

- PR Error: 30 m (Road) and 50 m (Urban)
- Doppler Error: 2 m/s (Road) and 3 m/s (Urban)

Firstly, a separated analysis of the performances provided by each indicator has been performed. The following tables show the PFA and PMD performances obtained for road (R) and urban (U) environments.

Multi-Antenna Indicator	Pseudorange			
	PFA		PMD	
	Road	Urban	Road	Urban
Availability of PR&DP SD	1%	1%	90%	90%
PR SD	4%	10-15%	35-70%	35%
Availability of CP SD	10%	20-25%	10-20%	40-50%
CP SD residual	2%	16%	80%	30-40%

Table 2- Performance of pseudorange error indicators

Multi-Antenna Indicator	Doppler			
	PFA		PMD	
	Road	Urban	Road	Urban
Availability of PR&DP SD	1%	1%	97%	97%
DP SD	10%	20-25%	0-10%	10%
Availability of CP SD	10%	20-25%	0-30%	0-15%
CP SD residual	2%	16%	70%	30-40%

Table 3- Performance of Doppler error indicators

The lower the PFA and PMD values in Table 2 and Table 3 the better. For each column the best values have been marked in green and the PFA that could be problematic have been marked in red. When analyzing the results it should be taken into account what a 100% would mean: for example the CP SD residual statistics (last row) have been computed over the available CP SD, and the availabilities of PR&DP and CP SD measurements have been computed over the number of pseudorange (or Doppler) measurements received with one single antenna (MASTER). Another thing to bear in mind is that the PFA and PMD values have been computed for each indicator independently, which means that the percentages cannot be added as one indicator could be marking part of the measurements marked by the other.

The following conclusions can be derived for each indicator:

- Availability of PR&DP SD: although PMD is very high PFA is 1% or less so it is worth using it.
- PR SD: PFA is low and although it has a medium PMD in road environment, the PMD in urban is good enough to recommend its use.
- DP SD: PMD is outstanding but PFA is high, it could be a problem if it is combined with other indicator that could increase the PFA even more (other option would be to increase the used DP SD thresholds to improve the PFA at the cost of degrading the PMD).
- Availability of CP SD: PMD performances are good with pseudoranges and very good with Doppler but PFA is high, it could be a problem if it is combined with other indicator and the PFA increases even more.
- CP SD residual: PMD performances are better in urban than in road environment which is good, while PFA is very low in road environment and could be reasonable in urban. It can only be tested with GPS. If combined with the availability of CP SD it should be taken into account that the PFA applies over the available CP SD which means that the whole PFA would be around 11.8% for road and 33-37% for urban.

Modified Availability of CP SD Indicator

Because of the high PFA of the availability of CP SD in urban environment, its behaviour has been analyzed combined with the PR SD and DP SD indicators. After applying the following three indicators: availability of PR&DP SD, PR SD and DP SD, a subset of measurements will remain and for some of them the CP SD will be available and for others not. Figure 25 and Figure 26 show the PR and Doppler error of those measurements that have passed the first three indicators but for which the CP SD is unavailable:

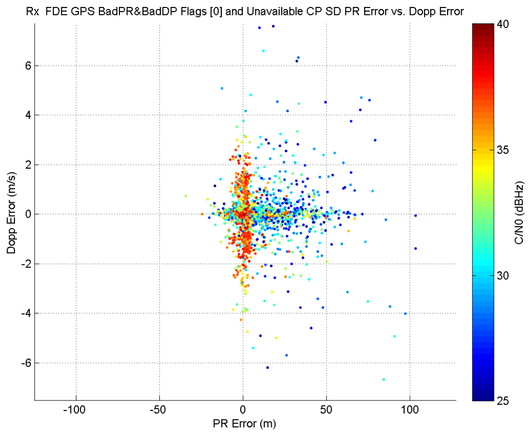

Figure 25- GPS PR and DP error of Unavailable CP SD after applying the three indicators [C/N0] - Urban

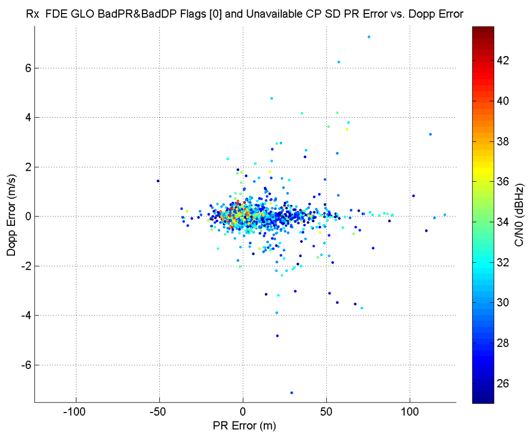

Figure 26- GLONASS PR and DP error of Unavailable CP SD after applying the three indicators [C/N0] - Urban

Hence, using the availability of CP SD indicator to discard measurements would mean that all the measurements represented in the previous graphics would be discarded, but looking at the C/N0 values (colours) one important aspect should be highlighted, the measurements with higher errors correspond to measurements with a C/N0 below 35 dBHz (blue, green and yellow points) but measurements with high C/N0 have lower errors, so these ones should not be discarded. The cause of this behaviour is supposed to be connected with differences in the quality of the signals received at the different antennas and also with the correlation between the quality parameters used to decide whether a measurement is valid or not (C/N0 for pseudorange and Doppler and $c2\phi_k$ for phase measurements). Its complete understanding would require future investigations. Nevertheless, the indicator employed in the FDE can take advantage of the observed behaviour.

In the light of the results, it makes sense to say that if the receiver cannot provide carrier phase measurements for signals with higher C/N0 that does not mean that the PR or Doppler measurement is a faulty one. Hence, the availability of CP SD indicator will be complemented with a C/N0 threshold and only those measurements with an unavailable CP SD and under the C/N0 threshold would be rejected. Thus the PFA would be improved from 20-25% in urban to 18-20% while maintaining the PMD.

Combinations of Indicators

As already mentioned, the different indicators can be combined and the best combination would depend on the navigation and integrity algorithm and how the flags are used in the algorithm. In order to assess the potential of the analyzed indicators different combinations will be tested. The criteria used to decide the combinations is based on the results obtained when the indicators were separately analyzed:

- The availability of PR&DP SD can be applied to all the combinations due to its very low PFA,
- The PR SD is only applied to PR measurements
- The DP SD is only applied to DP measurements
- The modified Availability of CP SD will be used taking into account a C/N0 threshold.
- The DP SD has a very good PMD but a high PFA so the CP SD residual indicator, which only applies to GPS, will only be used for PR meas. if used in combination with DP SD to avoid PFA degradation.

Bearing in mind the complexity of the different indicators, they can be sorted in increasing order of complexity as follows:

1) Availability of PR&DP SD, PR SD and DP SD: the receiver at each FE has to provide PR and DP meas.
2) Modified availability of CP SD: the receiver at each FE has to provide CP meas.
3) CP SD residuals (GPS): the receiver at each FE has to provide CP measurements; attitude information is needed to compute the residuals and to correct the bias; and the FEs should use a common clock. It would also be possible to use the CP DD residuals instead, they would not need a common clock but, as already explained, they are noisier than the SD.

Table 4 provides the indicators used by each of the four combinations that will be tested. There are simple ones like the first one (Pr&DpSD), which does not require CP measurements or the last one (AvCpSD), which is only based on the availability of measurements and does not require checking their differences. On the other hand, there is a combination (the third one) that includes almost all the indicators (CP SD residual indicator is only applied to GPS and requires an attitude estimation). Many other combinations would be possible but these four cover a wide range of possibilities and are enough to assess the potential of a multi-antenna FDE.

Multi-Antenna Indicator	Meas Type Marked by the Indicator	Combinations of Indicators: Pr&DpSD	Pr&DpSD + modAvCpSD	Pr&DpSD + modAvCpSD + CpSDResid	AvCpSD
Availability of PR&DP SD	PR	✓	✓	✓	✓
	Doppler	✓	✓	✓	✓
PR SD	PR	✓	✓	✓	—
	Doppler	—	—	—	—
DP SD	PR	—	—	—	—
	Doppler	✓	✓	✓	—
Modified Availability of CP SD using C/N0	PR	—	✓	✓	✓
	Doppler	—	✓	✓	✓
CP SD residual (GPS)	PR	—	—	✓	—
	Doppler	—	—	—	—

Table 4- Different Combinations of Multi-Antenna Indicators for an FDE

The following table shows a summary of the PFA and PMD performances at high error values obtained for the different combinations of indicators.

Multi-Antenna Combination of Indicators	Pseudorange PFA Road	Pseudorange PFA Urban	Pseudorange PMD Road	Pseudorange PMD Urban
Pr&DpSD	5%	15%	5-10%	5-15%
Pr&DpSD+modAvCpSD	10-15%	30%	1-5%	1-10%
Pr&DpSD+modAvCpSD +CpSDResid	10-15%	30-40%	1-5%	1-5%
AvCpSD	10-15%	25%	5%	20-35%

Table 5- Pseudorange PFA and PMD performances for Combinations of Multi-Antenna Indicators

Multi-Antenna Combination of Indicators	Doppler PFA Road	Doppler PFA Urban	Doppler PMD Road	Doppler PMD Urban
Pr&DpSD	10%	25%	0-5%	10%
Pr&DpSD+modAvCpSD	15%	30%	0-5%	1-5%
Pr&DpSD+modAvCpSD+ CpSDResid	15%	30%	0-5%	1-5%
AvCpSD	10-15%	25%	1-30%	1-10%

Table 6- Doppler PFA and PMD performances for Combinations of Multi-Antenna Indicators

Looking at the pseudorange PFA and PMD statistics there is no clear winner, while the best PFA performances are achieved by the first combination (Pr&DpSD) the second and the third have better PMD but with the drawback of having a worse PFA, which is very high in urban and could be problematic depending on the navigation algorithm.

Regarding Doppler results (second and third combinations are the same with respect to Doppler), the clear winner in road environment is the first combination (Pr&DpSD) but in urban the fourth one (AvCpSD) seems better than the first while the second and the third improve the PMD in exchange of degrading the PFA.

As noted before, the most complex indicator among the presented ones was the CpSDResid. Now the impact of the CpSDResid along with the other indicators will be assessed, comparing its results with the ones obtained with the second and the third combinations. There are no significant differences in road environment, just the expected ones due to the fewer amount of faulty measurements due to the environment. Regarding urban environment, the PMD improves from 10% to 2.5% at 50m at the cost of reducing the availability from 68.3% to 61.4%. As a conclusion, the combination using the CpSDResid provides the best PMD performances in urban environment at the cost of reducing the availability.

Impact on Accuracy of the Combinations of Indicators

Finally the following figures show the impact of the different combinations on the hybrid navigation algorithm in a road and in an urban scenario. Take into account that the flags generated by the different combinations of indicators have been used to exclude the pseudorange and Doppler measurements and that the same configuration of the navigation algorithm has been used in all cases.

<u>*Road HPE*</u>

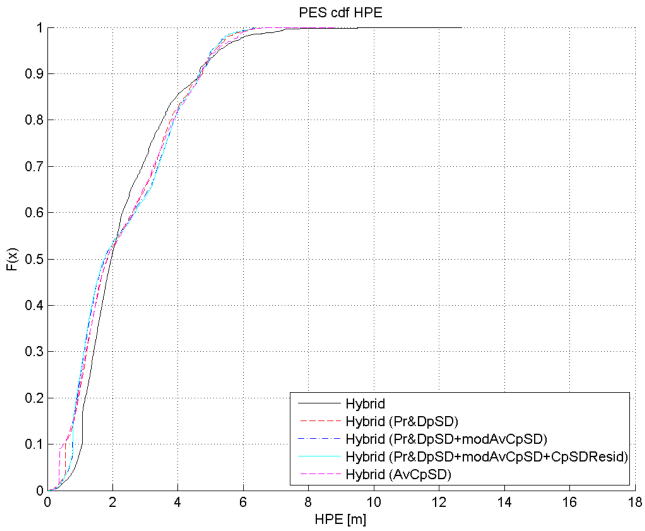

Figure 27- Impact of the Multi-Antenna FDE on the HPE using the Hybrid Algorithm - Road

Comparing the behaviour of the Hybrid algorithm without flags with the others, the graphic shows that applying the multi-antenna FDE flags does not have great impact on the statistics (except perhaps for the higher percentiles) and that the impact is similar for all the combinations:

- Percentiles between 0 and 50 are improved a few tens of cm (around 25% of the HPE are below 1 m).
- Percentiles between 60 and 85 are degraded a few tens of cm.
- The highest percentiles are improved, between 98 and 99 around one meter and the maximum HPE is reduced from 14.9 m to 6.3-9.8 m.

Giving importance to the reduction of the higher percentiles as it supposes an improvement in terms of maximum errors that can be experienced, all the combinations improve the Hybrid without flags statistics, being the first three combinations the ones giving the best performances.

<u>*Urban HPE*</u>

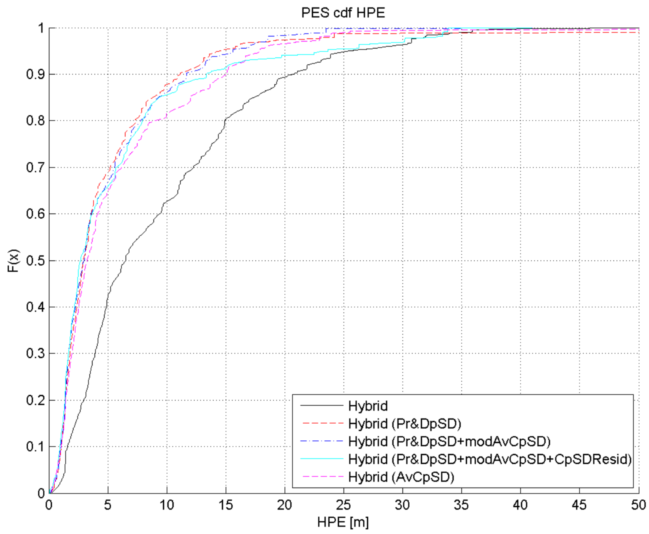

Figure 28- Impact of the Multi-Antenna FDE on the HPE using the Hybrid Algorithm - Urban

Analyzing the urban HPE, it can be seen that the results obtained with the Hybrid algorithm using the different multi-antenna FDE flags are considerably improved at all the percentiles, only between the 99 and 100 percentiles two of the FDEs, the simpler ones (Pr&DpSD and AvCpSD), are worse that the Hybrid algorithm without flags. The improvement is such that for example at percentile 50 the error passes from 6 to 3 m, at percentile 70 from 12 to 5-6 m and at percentile 90 from 20 to 11-15 m.

Two of the FDEs are always better than the Hybrid reference, the best one is Pr&DpSD+modAvCpSD and Pr&DpSD+modAvCpSD+CpSDResid is the second.

If one combination of multi-antenna indicators should be selected as an FDE for this hybrid navigation algorithm and if this FDE is aimed to work in both, road and urban environments, then the choice would be the Pr&DpSD+modAvCpSD combination (see the indicators used by this combination in Table 4). The second one would be Pr&DpSD+modAvCpSD+CpSDResid, this combination uses the same indicators as the previous one plus the CpSDResid, which improves the PMD performance but with a reduction in availability leading to slightly worse performances.

Nevertheless, it should be taken into account that with other navigation algorithm or with the same algorithm but downweighting the flagged measurements instead of rejecting them, the best performances could be provided by a different combination of indicators. The important conclusion is that a multi-antenna FDE is useful for improving the performances in urban environments.

SPOOFING DETECTION

When a receiver is spoofed by one single source all the signals will arrive from the same direction and in such situation the carrier phase single differences for all the satellites will have similar values at each baseline, so the presence of a spoofer can be detected by comparing the CP SD between satellites at both baselines, which is the same as making CP DD between satellites.

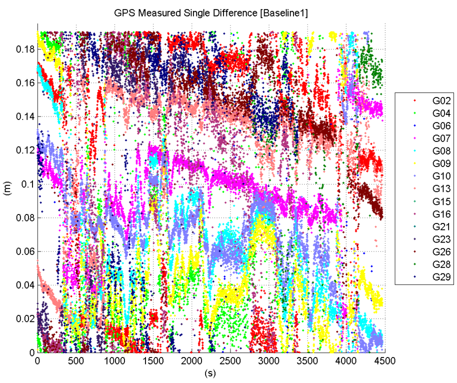

Figure 29- Measured CP SD (wavelength module) - Road

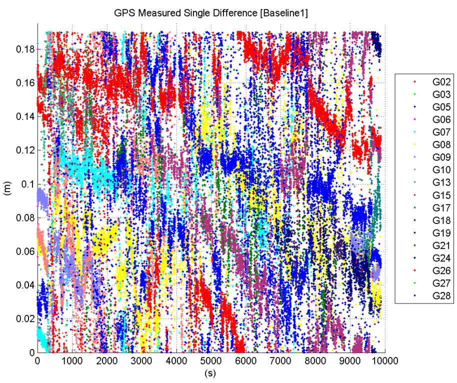

Figure 30- Measured CP SD (wavelength module) - Urban

Figure 29 and Figure 30 provide an example of the CP SD (the fractional part: λ-module) measured in road and urban environments and Figure 31 shows the CP SD measured in a test where all the signals were coming from the same direction. By comparing the graphics it can clearly be noticed that there is a radical change in the λ-module of the measured CP SD when the signals are being spoofed.

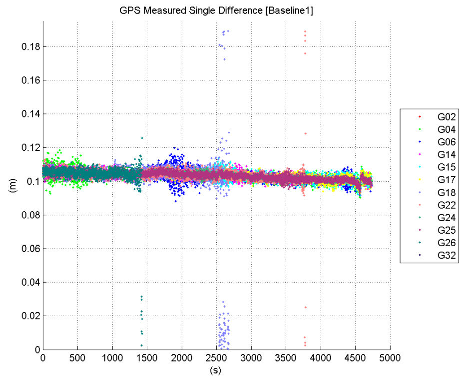

Figure 31- Measured CP SD (λ-module) - JRC Anechoic Chamber (spoofing-like scenario)

A metric can be defined to measure the “distance” between two satellites, like the Root Mean Square (RMS) of the difference of phase SD between two satellites (i.e. CP DD) at the different baselines. If the RMS of the CP DD at both baselines is below a threshold then both satellites are considered to arrive from the same direction. In order to evaluate if one satellite is being spoofed, the number of satellites coming from the same direction as the satellite under analysis is checked and if it is above certain percentage of the satellites then it is considered to be potentially spoofed and if, after checking all the satellites, most of them (more than a certain percentage) are marked as spoofed then the spoofing flag is raised at that epoch. Obviously, a minimum number of tracked satellites are needed to carry out the percentage check. Thus, this simple algorithm, which does not require any previous knowledge of the attitude or any calibration, can detect the presence of a spoofer trying to deceive the receiver.

This snapshot algorithm is versatile enough as the threshold used to check the CP DD can be configured according to the environment (it could be adapted in real time according to the detected noise) and also because the spoofing flag is raised using a configurable minimum percentage of satellites coming from the same direction, this means that even if the spoofer only replaces part of the satellites it can also be detected.

The spoofing scenario employed in this test is not a completely realistic one as it was carried out inside an anechoic chamber thus presenting very low multipath. Having been carried out with a real spoofer in road or urban environments the noise would have increased to the same level observed when analysing the CP SD in those environments. This means that, assuming that the threshold used to check the CP DD is in line with the environment, it is completely feasible to detect the spoofer.

As an example, Table 7 shows how the algorithm, configured to raise the spoofing flags when the percentage of satellites coming from the same direction is above 66% (assuming the spoofer would not replace all the satellites), does not have any false alarm in real road environment and only a few (~1%) false alarm epochs in the urban scenario (it could be improved with a small increment of the percentage threshold). As expected, it completely detects spoofing in the scenario recorded at the JRC within the anechoic chamber and one single source of GPS signals (spoofer).

Scenario	Total Epochs	Epochs with enough SV (>=3) to check spoofing	Epochs when spoofing has been detected
Road	4467	4461	1 (0.02%)
Urban	7110	5850	65 (1.1%)
JRC Anechoic Chamber (spoofing scenario)	4735	4733	4733 (100%)

Table 7- Spoofing Detection Results

The presented spoofing detection algorithm is completely valid for meaconing scenarios or when only one single spoofer is present, but it has limitations. If the spoofing attack is more complex and several spoofers are used, each one transmitting a different subset of satellites, then the spoofing attack could be successfully detected by lowering the percentage threshold but the consequence is that for low percentages the false alarms will increase to an unacceptable level. The following figure provides the false alarm rates obtained for different percentage thresholds in road and urban scenarios:

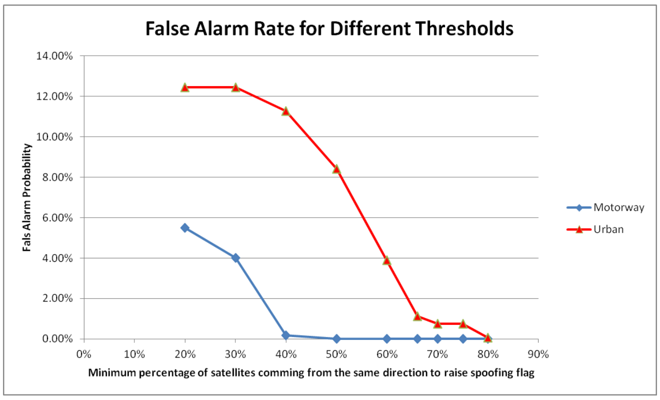

Figure 32- False Alarm in Spoofing Detection

This means that in motorway/road environment two spoofers could be detected by the tested snapshot algorithm with an acceptable false alarm rate but with three or more spoofers in road environment or with two or more spoofers in urban this algorithm will provide very high false alarm rates degrading the availability. The solution to cope with these cases is to introduce more complexity in the spoofing detection algorithm.

The tested algorithm is snapshot (previous epochs are not taken into account), which matches with a Time to Alarm (TTA) of 1 second, but the TTA requirement could be several seconds (it would depend on the application). So a first step could be to take into account the last N seconds before raising an alarm, being N the TTA, thus the false alarm. For example, it has been tested that taking the last 8 epochs and raising the spoofing alarm if at 5 or more epochs the snapshot algorithm detects spoofing, improves the false alarm for a 50% threshold in urban from 8.4% to 3.6% and, following the binomial distribution, the overall detection probability also improves for snapshot detection probabilities above 80%.

However, the problem when the number of spoofing sources increases to three or more is that the environment leads to a situation where their presence cannot be easily differentiated from a non-spoofed situation, moreover in urban environment, where the noise is higher, there are less number of satellites in view and phase measurements are less available. Then, in case numerous spoofers need to be detected, one solution is to reduce the noise. This could be done for example by using gyroscopes to average the CP SD measures obtained at different epochs. Other solution could be to increase the number of antennas and average measures between them.

Also, a more complex algorithm could get advantage of the knowledge of the actual line of sights provided by the navigation message (which could be obtained through an assisted channel to avoid using the spoofed one) checking if the CP DD and CP SD of the received signals are coherent with them. This algorithm would be an adaptation of an attitude estimation algorithm based on CP DD and CP SD measurements (CP DD are noisier but CP SD measurements are affected by a slowly varying common bias). This kind of solution would be the one needed in worst case scenarios where each spoofer is replacing one single satellite, each one arriving from a different direction.

On the other hand, it has been assumed that the spoofing detection algorithm needs to work with no previous knowledge of the attitude but, if this would be not the case due to the application characteristics and there is an available estimation of the attitude (not affected by the spoofing attack), then the CP DD and/or CP SD residuals can be computed, as explained in previous sections, and those signals not arriving from the expected direction (residuals above a certain threshold) would be identified as spoofing signals their residuals would be above the detection threshold. Again, the noise plays an important role, CP SD measurements have lower noise than CP DD ones but they need to estimate a very slowly varying common bias, which should not be updated with the spoofing signals (not with the residuals above the threshold). A spoofing attack like in the worst case scenario previously described, will be detected as most part of the signals will be above the threshold and, if only part of the signals are spoofed, most of them will be detected and only a few ones would remain and pass to the navigation algorithm where could be rejected (easily if the navigation algorithm is aided by external sensors).

Besides, under certain conditions (with calibrated CP SD) it would be possible to find out the DoA of the spoofing signal (i.e. elevation and azimuth). Once the CP SD are calibrated, which means to estimate the bias common to all the CP SD measurements, if a spoofer starts transmitting, then its azimuth and elevation could be estimated which could help to locate the source. Of course, as the angle estimation is based on the previous estimation of the bias common to all the CP SD and this bias should not be updated during a spoofing attack, the angle estimations will be valid as long as the value used to correct the CP SD is valid. As it has been observed, the bias varies very slowly so the angle estimation will degrade with time. If the value used to correct the CP SD is just the last estimated bias then, with the worst observed drift, after 10 minutes the angle estimations would have deviations of 10-20º, on the other hand, as the behaviour of the bias has been observed to have a very slowly varying drift, if the drift is also estimated in the calibration and used to propagate the bias when the spoofing attack is detected then the estimated angles could be valid for one or two hours.

In the end, like it happens with the countermeasures and counter-countermeasures in electronic warefare, each step increasing the complexity of the attack/defence can be overcome by a more complex defence/attack, until there is an effort/cost or technical limit that makes last step not feasible. The objective of spoofing detection is to put enough barriers so that only extremely complex spoofing attacks could succeed and the multi-antenna technology has shown the capability of playing a key role in spoofing detection.

The conclusion is that the three-antenna Front-End with the presented snapshot spoofing detection algorithm can be used to successfully detect the presence of up to two spoofers depending on the environment and the TTA without any calibration and without using any other input information (attitude is not needed to detect spoofing). Also, it has been analysed how this technology could be evolved to detect more complex spoofing attacks.

CONCLUSIONS

The study presented in this paper has provided an overview of the different techniques at PVT level that can be applied when using measurements from a mass-market level multi-antenna receiver in order to deal with threats affecting the provision of reliable positioning services, like NLoS or spoofing. The techniques have been tested with real data collected in urban and road environments (urban routes include street canyons where NLoS signals appear more frequently) so the provided performances are representative of what can be achieved in real situations.
The employed data collection platform uses a dedicated equipment to obtain the truth reference trajectory and attitude needed to assess the errors and the impact of these techniques into the navigation performances.

The most important aspect in the paper is that it shows how the techniques tested with real data helped in the detection of NLoS signals and are also capable of detecting the presence of spoofing signals, two critical threats in the provision of reliable positioning services.

The performed analysis about the capabilities that can be provided by a three-Antenna FE with a common clock has demonstrated that:

- The multi-antenna carrier phase differences can be used to check if the received signals are coming from the right direction, which turns it into a valid indicator for detecting high error measurements, but in contrast this indicator has a high PFA in urban environment.
- The multi-antenna FE is able to estimate the angle of arrival of the received signals in road environment and also in urban environment but with degraded availability.
- The measurements provided by a multi-antenna FE can be used by an FDE to improve the HPE performances. A great improvement is achieved in urban where HPEs decrease by a factor of 2.
- The best combination of indicators for the FDE depends on the navigation algorithm and on how it uses the FDE flags.
- The multi-antenna FE is capable of detecting the presence of a spoofer.

The analysis made in this paper about the multi-antenna possibilities gives an idea of what can be achieved with it so each user application, according to its requirements, can decide if it is worth to use a multi-antenna receiver according to the improvement that it provides.

REFERENCES

[1] E. Domínguez et al. “Characterization of Integrity Threats in Terrestrial Applications Using Real Signal Captures”, ION GNSS+ 2014.

[2] SRX-TRITON Multi-Antenna Front-End: http://www.gmv.com/en/space/products/srx-10/Front-end/

[3] srx-10 SW Defined Multi-Constellation GNSS Receiver: http://www.gmv.com/en/space/products/srx-10

[4] Elliott D. Kaplan and Christopher J. Hegarty “Understanding GPS Principles and Applications”, second edition, Ed. Artech House.

[5] Bradford W. Parkinson and James J. Spilker Jr. “Global Positioning System: Theory and Applications Volume I”, Published by the American Institute of Aeronautics and Astronautics, Inc.